Combustion and Flame 194 (2018) 343–351

Contents lists available at ScienceDirect

Combustion and Flame

journal homepage: www.elsevier.com/locate/combustflame

Broken C-shaped extinction curve and near-limit flame behaviors of low Lewis number counterflow flames under microgravity

Tomoya Okuno[a,*], Takaki Akiba[a], Hisashi Nakamura[a], Roman Fursenko[b], Sergey Minaev[b], Takuya Tezuka[a], Susumu Hasegawa[a], Masao Kikuchi[c], Kaoru Maruta[a,b]

[a] Institute of Fluid Science, Tohoku University, 2-1-1 Katahira, Aoba-ku, Sendai, Miyagi 980-8577, Japan.
[b] Far Eastern Federal University, 8 Suhanova St., Vladivostok, 690950, Russia
[c] Japanese Aerospace Exploration Agency, 2-1-1 Sengen, Tsukuba, Ibaraki 305-8505, Japan

ARTICLE INFO

Article history:
Received 24 November 2017
Revised 31 January 2018
Accepted 14 May 2018

Keywords:
Counterflow premixed flames
Flame ball
Radiative extinction
Flammability limit
Microgravity combustion

ABSTRACT

To examine the effect of Lewis number on the extinction boundary, flame regimes, and the formation of sporadic flames, microgravity experiments on counterflow flames for $CH_4/O_2/Kr$ ($Le \approx 0.7$–0.8) and $CH_4/O_2/Xe$ ($Le \approx 0.5$) mixtures, and three types of computations, which are one-dimensional computations with a PREMIX-based code using detailed chemistry, and three- and one-dimensional computations with the thermal-diffusion model using an overall one-step reaction were conducted. In the microgravity experiments, planar flames, planar flames with propagating edges, planar flames with receding edges, star-shaped flames, cellular flames, and sporadic flames were identified, and their regions of existence in the equivalence ratio-stretch rate plane were obtained. Sporadic flames were formed for Xe mixtures but not for Kr mixtures in the experiments. Similarly, sporadic flames were formed at $Le = 0.50$ but not at $Le = 0.75$ in the three-dimensional computations with the thermal-diffusion model. Also, the flame regime of sporadic flames extended far beyond the extinction boundaries obtained in the one-dimensional computations in both experiments and the three-dimensional computations. Furthermore, a comparison of the sporadic flames and flame balls in the three-dimensional computations showed that sporadic flames are intermediate combustion modes that segue flame balls to propagating flames.

1. Introduction

Studies on the dynamics and the combustion limits of premixed flames are essential fundamentals for the development of clean combustion technologies such as lean-burn engines. However, a complete and comprehensive understanding on the dynamics and the combustion limits of near-limit stretched premixed flames has not yet been achieved for low Lewis numbers, despite extensive efforts of many researchers. The combustion limits of stretched premixed flames have been widely studied using flames in stagnation flow or counterflow fields [1–10]. Experimental investigations on the combustion limits at low stretch rates have been conducted under microgravity [7,9,10], in order to minimize disturbance to the flame caused by natural convection. These studies have been conducted over a range of Lewis numbers, *Le*, from 0.97 to 1.8, but studies for even lower Lewis numbers are still scarce.

Focusing on this issue, we have previously conducted counterflow experiments under microgravity using $CH_4/O_2/Xe$ mixtures ($Le \approx 0.5$) at stretch rates from 1.1 to 4.4 s^{-1} [11–13]. We have also conducted experimental investigations under microgravity with the effect of radiation reabsorption at slightly higher Lewis numbers ($Le \approx 0.75$) using $CH_4/O_2/CO_2$ mixtures [14]. In these previous studies, we have shown that transitions to ball-like flames from counterflow planar flames occur at extremely low stretch rates [11–14]. Extension of the combustion limit due to the formation of multiple ball-like flames, termed sporadic flames, has also been obtained in the framework of the thermal diffusion model [13]. Sporadic flames are a group of ball-like flames, which are formed when each cap-like segment in a cellular flame breaks up and close upon themselves [15–18]. Similar flames have also been reported to exist in uniform flows [15–21], tubes [22–25], divergent channels [26], and Hele–Shaw cells [27]. However, the difficulty in experimental observation of these flames which are free from the effect of conductive heat loss or disturbance from natural convection has resulted in incomplete studies on these sporadic flames. Namely, the effects of Lewis number on the combustion limits, formation of sporadic flames, and flame regimes under microgravity remain largely uninvestigated. Therefore in this study, we aim to investigate this issue by using Kr or Xe gas as a diluent for methane and oxygen mixture to change the Lewis number.

* Corresponding author.
E-mail address: okuno@edyn.ifs.tohoku.ac.jp (T. Okuno).

https://doi.org/10.1016/j.combustflame.2018.05.014

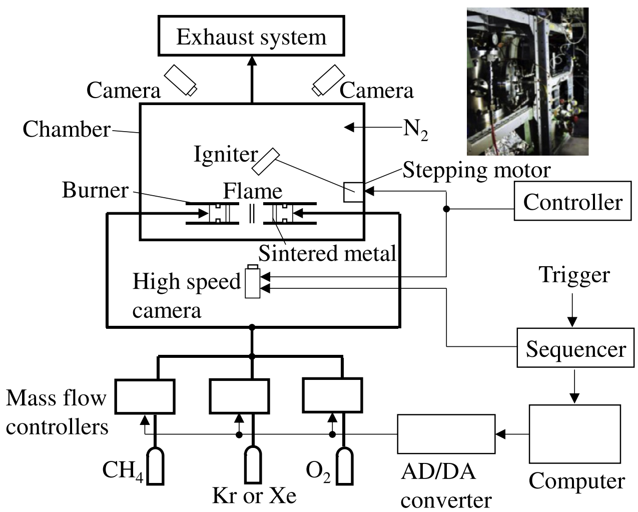

Fig. 1. Schematic and a picture of the experimental setup [7].

Another type of flame that can be observed under microgravity is the flame ball. Flame balls are spherical flames without flame propagation which exist in quiescent mixtures at Lewis numbers sufficiently lower than unity. The existence of flame balls were first suggested by Zel'dovich [28] and was later verified by theoretical [29–31], computational [32–35], and experimental [36,37] investigations. A single ball-like flame in the sporadic flame resemble these flame balls in shape and in the conditions that these flames are formed. However, direct comparisons between the sporadic flames and the flame balls have not been conducted yet. Therefore in this study, we have additionally compared the flame structures, characteristic flame sizes, and the combustion limits of flame balls and the sporadic flames obtained with computations in an attempt to clarify the relation between these two flames.

2. Experimental methods

Microgravity experiments were conducted to obtain the combustion limit, near-limit extinction boundary, and flame regimes of counterflow flames for mixtures with different Lewis numbers. Figure 1 shows a schematic of the experimental apparatus.

The microgravity environment was attained by parabolic flights of an airplane (MU-300) operated by Diamond Air Service Incorporation [38], Japan. The duration of microgravity was around 15–20 s, and the gravity levels were on the order of ± 0.01 G. In the present study, data were removed for consideration when the gravity level exceeded 0.1 G during the microgravity experiments. To conduct the counterflow flame experiments, two opposed cylindrical burners were placed inside a chamber. Here, the burner inner diameter was 30 mm and the burner distance was from 30 to 45 mm. The burner distance was changed depending on the stretch rate to avoid upstream conductive heat loss to the burners from the flames. A detailed description of the experimental apparatus and the experimental procedure can be found in [7].

In the experiments, $CH_4/O_2/Kr$ or $CH_4/O_2/Xe$ premixtures were supplied to both burners, forming a counterflow field. The mole fraction ratio of O_2 to the diluents in the mixtures were set to 0.14. Lewis numbers for Xe and Kr mixtures were around 0.5 and 0.7–0.8, respectively. Separate mass flow controllers were used to control the flow rates for each gas component of the mixtures. Each mass flow controller was calibrated before and after each flight using a flow meter (Horiba SF-1 U) to ensure that no changes in the applied voltage-flow rate conversion factor occurs due to the acceleration during the flight. The accuracy of the flow meter measurement is within $\pm 1.0\%$ of the reading point. This results in around $\pm 2.0\%$ uncertainty in the equivalence ratio and $\pm 1.0\%$ uncertainty in the stretch rate.

After ignition, the equivalence ratio ϕ and/or the stretch rate a were gradually changed to obtain extinction. Here, the global stretch rate was defined as $a = 2U/L$ where U is the mean velocity at the burner outlet and L is the burner distance. In most cases, the stretch rate was kept constant and the equivalence ratio, ϕ, was gradually decreased by 0.015 per second. For flame observation, two HD cameras and a high-speed camera equipped with an image intensifier (Photron FASTCAM MC2.1) were used. Equivalence ratio at extinction was defined as the instantaneous equivalence ratio when the chemiluminescence from flames vanished in the camera image by considering flow residence time from mass flow controllers to the counterflow field. To check the effect of the G-jitter, counterflow flame extinction experiments using CH_4/air mixtures were conducted, and a good agreement between the extinction boundaries obtained with the droptower and the airplane experiments were found. Supplementary video files of the droptower and airplane experiments are also provided to demonstrate the small effect of the G-jitter.

3. Computational methods

We have conducted three types of computations in this study: one-dimensional computations with a PREMIX-based code using detailed chemistry, and three- and one-dimensional computations with the thermal-diffusion model using an overall one-step reaction.

One-dimensional computations with a PREMIX-based code using detailed chemistry for ideal steady-state planar counterflow flames [10] were conducted to obtain the C-shaped extinction boundary and their results were compared with the experimental results. The optically thin model was used for the radiation heat loss from the flames to the ambient [10]. All computations were conducted under atmospheric pressure. GRI-Mech 3.0 [39] without nitrogen reactions was used for the chemical mechanism. Thermodynamic [40] and transport [41] properties for Xe and Kr were added, and the third-body collision coefficients of Ar were used for Xe and Kr. GRI-Mech 3.0 without nitrogen reactions including Xe was used for $CH_4/O_2/Xe$ mixtures in [42], and sufficiently accurate results were obtained even at equivalence ratios near the lean combustion limit. From this, similar accuracy is expected for $CH_4/O_2/Kr$ mixtures due to the similar molecular structure between Kr and Xe. Computations using the same chemical mechanism showed that the flame temperatures of Kr and Xe flames were 1462 and 1448 K, respectively, and the flame propagation velocities of Kr and Xe flames were 3.58 and 2.62 cm/s, respectively, at $\phi = 0.62$ for the radiative planar unstretched flame.

Three-dimensional computations with the thermal-diffusion model and an overall one-step reaction for counterflow flames used in [13] were employed to obtain the flame regimes and to qualitatively compare with the experimental flame regimes. Here, transient non-dimensional equations describing the fuel concentration and the temperature [13] were solved with the constant density assumption and a given flow field, and the governing equations are as follows.

$$\frac{\partial T}{\partial t} + \vec{V}\nabla T = \nabla^2 T - h\left(T^4 - \sigma^4\right) + (1-\sigma)W(T,C) \quad (1)$$

$$\frac{\partial C}{\partial t} + \vec{V}\nabla C = Le^{-1}\nabla^2 C - W(T,C) \quad (2)$$

The units for temperature, T, and the fuel concentration, C, are the adiabatic flame temperature, T_b, and the initial gas concentration, C_0, respectively. The unit for the distance is the flame